Spectral changes in Si-O-Si stretch band of porous glass network upon ingress of water

Huseyin Kaya[1], Dien Ngo[2], Stéphane Gin[3] and Seong H. Kim[1,2*]

1. Department of Materials Science and Engineering, The Pennsylvania State University, University Park, 16802, USA
2. Department of Chemical Engineering and Materials Research Institute, The Pennsylvania State University, University Park, PA 16802, USA
3. CEA, DEN, DE2D, SEVT, Bagnols-sur-Ceze F-30207, France

*Corresponding author: shkim@engr.psu.edu

Abstract: Water ingress into porous glass can induce internal stress, resulting in strains in chemical bonds of the network. For silica and silicate glasses, the position of Si-O-Si stretch mode in infrared spectroscopy is known to vary with the degree of strain in the Si-O network. Then, one could hypothesize that this stress due to water ingress could be probed with infrared spectroscopy. We tested this hypothesis using porous layers formed through aqueous corrosion on a model nuclear waste glass. The porosity and thickness of the porous layer were determined using ellipsometry. The humidity-dependent infrared spectra of the samples showed a red-shift of the Si-O-Si stretch band; however, it was difficult to deconvolute the spectral change due to variation of effective refractive index of the sample upon water ingress. Thus, it was infeasible to unambiguously determine the internal stress of porous glass network upon water ingress using the infrared method alone.

Introduction

Water ingress into glass can drastically change the chemical and mechanical properties of glass.[1, 2] The dissociation of the Si-O-Si bridging bonds of the glass network by reactions with water molecules diffusing into the glass can also induce internal stress to the glass network.[3, 4] Porous surface layers can be formed through leaching of mobile network modifier ions or incongruent dissolution of network formers upon aqueous corrosion.[5-7] If the glass surface layer is porous (Figure 1), then water ingress can occur more readily,[8, 9] which often can be accompanied by swelling of the porous network due to changes in surface energy.[10-12] Since the bulk glass would not swell, the water-induced swelling of the porous surface layer could produce a large stress gradient at/near the interface between the surface layer and the bulk.[8, 9] Thus, the capability of measuring the internal stress induced by the ingress of water into the glass surface is necessary for better understanding of how water uptake alters the surface properties of glass.

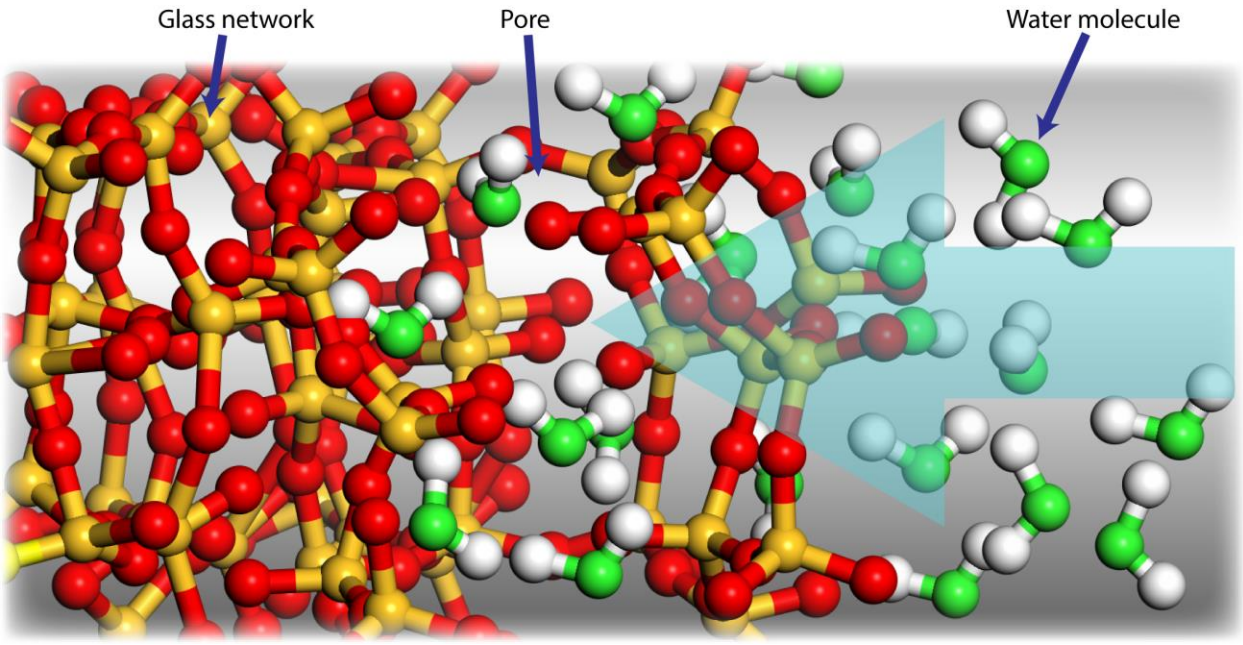

Figure 1. Schematic illustration of water ingress into porous SiO_2 glass network.

The physical swelling of the porous glass network is inevitably associated with strains in the chemical bonds of the glass network. Such strains can alter the vibrational spectral features of the glass network. In fact, it is known that for silica and silicate glasses, application of compressive or tensile stress can induce a red- or blue-shift of the peak position of the stretch band of the Si-O-Si bridging oxygen (BO), $\nu_{Si\text{-}O\text{-}Si}$, in the 1050-1100 cm^{-1} region of the infrared (IR) spectrum of glass.[13-19] Similarly, creation of compressive stress in the subsurface region of glass through exchange of network modifier ions with bigger ions also induces the red-shift of the BO stretch band in the IR spectrum.[20-22] The band position shift has been attributed to the change in the Si-O-Si dihedral bond angle through the non-central force constant model which was derived by applying the equation of motion principles to a simple molecular cluster model with certain assumptions.[23-25] Recently, more realistic and assumption-free interpretation was proposed through theoretical calculations of the dielectric constant, refractive index, and vibrational spectrum of silica glass using molecular dynamics (MD) simulations.[26] This new interpretation correlates the BO stretch band position to the Si-O bond length distribution in the glass network. Then, a question arises if the same spectral interpretation rule can be employed to measure or estimate the degree of network strain or the alteration of bond parameter distributions in the porous glass network upon uptake of water molecules.

Here, it should be noted that variations in the IR spectrum of a porous glass network can also occur due to a change in the effective refractive index upon ‘space filling’ of internal pores with water molecules.[27] Without distinguishing or deconvoluting this refractive index effect, one cannot attribute the observed BO stretch band shift merely to the strain of the glass network bonds. This study investigates how the refractive index change of a porous glass network upon water uptake is manifested in specular-reflection infrared (SR-IR) spectrum of the glass. A model

nuclear waste glass called International Simple Glass (ISG; 60.2 SiO_2, 16.0 B_2O_3, 12.6 Na_2O, 5.7 CaO, 3.8 Al_2O_3 and 1.7 ZrO_2 in mol%) [28] was chosen for this study because adsorption-induced stress might alter the chemical durability of corroded ISG surfaces which is of interest to the nuclear waste management community. The porous surface layer was produced through aqueous corrosion at 90°C in a pH 7 aqueous solution initially saturated with soluble silica species for 7 days and 209 days. The porosity and thickness of this altered surface layer were determined using a spectroscopic ellipsometry (SE) method.[29] Upon absorption of water into the porous alteration layer, we observed changes in the spectral shape of the $\nu_{Si\text{-}O\text{-}Si}$ band in SR-IR; however, it was also found that the similar changes could originate from the variation of effective refractive index upon filling the pores with water. This result showed that without taking into account the effective refractive index of the alteration layer accurately, it would be difficult to confidently assign the SR-IR spectral change observed upon water uptake in the porous surface layer to the swelling or internal stress of the layer.

Experimental methods

ISG coupons (2 cm × 2 cm × 0.1 cm) were cut from an ISG block (MoSci Corp.). One face of the coupon was polished to an optical finish, and the opposite side was left as-cut and rough to prevent the interference from the back reflection in SE measurements. The coupons were corroded in a static mode at pH 7.0±0.5 and 90 °C in aqueous solution initially saturated with soluble silica species prepared by following the protocol provided by Gin et al[5]. This solution contains ~5 mmol/L of soluble silicon-containing species and ~0.17 mmol/L of K^+ ions. Under these conditions, B and Na are leached out leaving behind a nanoporous gel-like layer mostly made of SiO_2, Al_2O_3 and ZrO_2. A porous Vycor glass coupon with 28% porosity [30], provided by Corning

Inc., was used as a reference sample for comparison. The Vycor glass has pores throughout the entire sample in the bulk, and the pore size varies roughly from 3 nm to 4 nm.[31] The Vycor glass was polished to an optical finish then cleaned by boiling in hydrogen peroxide (EMD Millipore) and sonicating in copious amounts of acetone (Honeywell Burdick & Jackson) and 200 proof ethanol (Decon Labs).

A spectroscopic ellipsometer (J.A. Woollam Co. Alpha-SE) with a wavelength range of 381–893 nm and CompleteEASE software package (J.A. Woollam Co.) were used to determine the alteration layer thickness and porosity and measure the adsorption-desorption isotherm of water at room temperature. The solid volume fraction and the porosity in the alteration layer of corroded ISG samples were determined from measurements at 0% relative humidity (RH). Assuming the solid volume fraction and thickness of the alteration layer do not change with water absorption into the internal pore, the water fraction in the alteration layer was determined from SE measured at higher RH conditions. If type-IV adsorption isotherm behavior is observed which is characteristic for adsorption in meso-porous materials with pore diameters between 2 and 50 nm,[32] the pore size distribution can be calculated using the Kelvin equation:[33]

$$\ln\frac{P}{P_o} = -\frac{1}{r_m}\frac{2\gamma V_L}{RT}\cos\theta \qquad (1)$$

where $\frac{P}{P_o}$ is relative humidity level, r_m is the radius of the meniscus, γ and V_L are the surface tension and the molar volume of water, θ is the water contact angle, R is the gas constant, and T is temperature. The present study assumes the pores in the alteration layer to be cylindrical and θ to be 0^o. These assumptions then lead to r_m to be equal to the pore radius, r_k, which is half of the pore diameter, d_k. Details of the ellipsometry analysis can be found in a previous work.[29]

The uptake of molecular water from the ambient air was confirmed through the attenuated total reflection infrared (ATR-IR) spectroscopy analysis using a Vertex80 FT-IR spectrometer equipped with an ATR accessory (DiaMaxATR; Harrick Scientific Products) which has a diamond crystal and an incident angle of 45^{o}. The acquired spectra are average of 100 scans with a resolution of 4 cm^{-1}.

SR-IR measurements were conducted using a Bruker Hyperion 3000 FT-IR spectrometer equipped with a reflective objective lens. This lens gave an IR incident and reflection angle of 18° from the surface normal and the analyzed area was 100 μm × 100 μm. A spectrum of gold surface was used as a reference. Spectra were obtained by averaging 400 scans with a resolution of 6 cm^{-1}. The samples were measured in a stainless-steel vessel containing a gas inlet covered with microscope slides on the top except an opening to permit IR beam. The RH-controlled gas was continuously flowed through the vessel. The RH level of the sample environment was controlled by adjusting the flow rates of the dry and water-vapor-saturated nitrogen streams. The RH of the sample environment was verified with a hygrometer (Omega Engineering Inc., RHXL3SD). The maximum IR peak positions were determined by fitting the data of the maximum intensity region (~20 cm^{-1} region near the peak position) with a fourth-order polynomial function.

The refractive index change of the porous glass network upon water uptake can be modeled with the Bruggeman effective medium approximation (EMA) method.[34] Assuming the second phase (void) is evenly distributed inside the matrix of the first phase (glass), the EMA approximation is expressed as:[35]

$$f_g \frac{\varepsilon_g - \varepsilon}{\varepsilon_g - 2\varepsilon} + (1 - f_g) \frac{\varepsilon_v - \varepsilon}{\varepsilon_v - 2\varepsilon} = 0 \quad (2)$$

where ε_g and ε_v are the dielectric constants of the glass (g) and void (v) components, f_g is the solid volume fraction, and ε is the effective dielectric constant of the porous medium. In theoretically-calculated SR-IR spectra of a medium consisting of 72% silica and 28% pores, ε_g of fused silica[36] was used. As water fills up the void space, ε_v can be replaced from the dielectric constant of air to that of water. Once the effective dielectric constant of the medium ($\varepsilon = \varepsilon_1 + i\varepsilon_2$) is determined, the refractive index ($n + ik$) of the composite system is calculated as following:

$$n = \left\{\left[(\varepsilon_1^2 + \varepsilon_2^2)^{\frac{1}{2}} + \varepsilon_1\right]/2\right\}^{1/2} \quad (3)$$

$$k = \left\{\left[(\varepsilon_1^2 + \varepsilon_2^2)^{\frac{1}{2}} - \varepsilon_1\right]/2\right\}^{1/2} \quad (4)$$

Then, the theoretical SR-IR spectrum can be generated with the Fresnel coefficient equations using the complex refractive index.[37]

Results and Discussion

The SE data of the 7-day and 209-day corroded ISG samples collected in dry condition (0% RH) are shown in Figure 2. The SE data were modelled with four sublayers and the total thickness of the alteration layer was determined to be ~726 nm and ~1614 nm for the 7-day and 209-day corroded ISG samples, respectively. These values are in good agreement with the results from secondary ion mass spectroscopy (SIMS) depth profiling and the mass balance of solution concentration of the leached species (Figure SI 4 of Ref. [5]).[5] The main parts (L_3 in Figures 2b and 2d) of the alteration layers are found to contain about 16.6% and 17.8% porosity, respectively. The interface region between the alteration layer and the bulk glass (L_1 and L_2) appears to be less porous than the main part of the alteration layer; this could be due to the roughness of the reactive

interface between the alteration layer and the bulk. Although the porosity in Figures 2b and 2d changes stepwise, it must vary gradually from the bulk to the main part of the alteration layer; the stepwise change is just an artifact in the optical fitting of the data with the minimum number of parameters. The large porosity of the exterior region (L_4) is an outcome of convolution with surface roughness.[38]

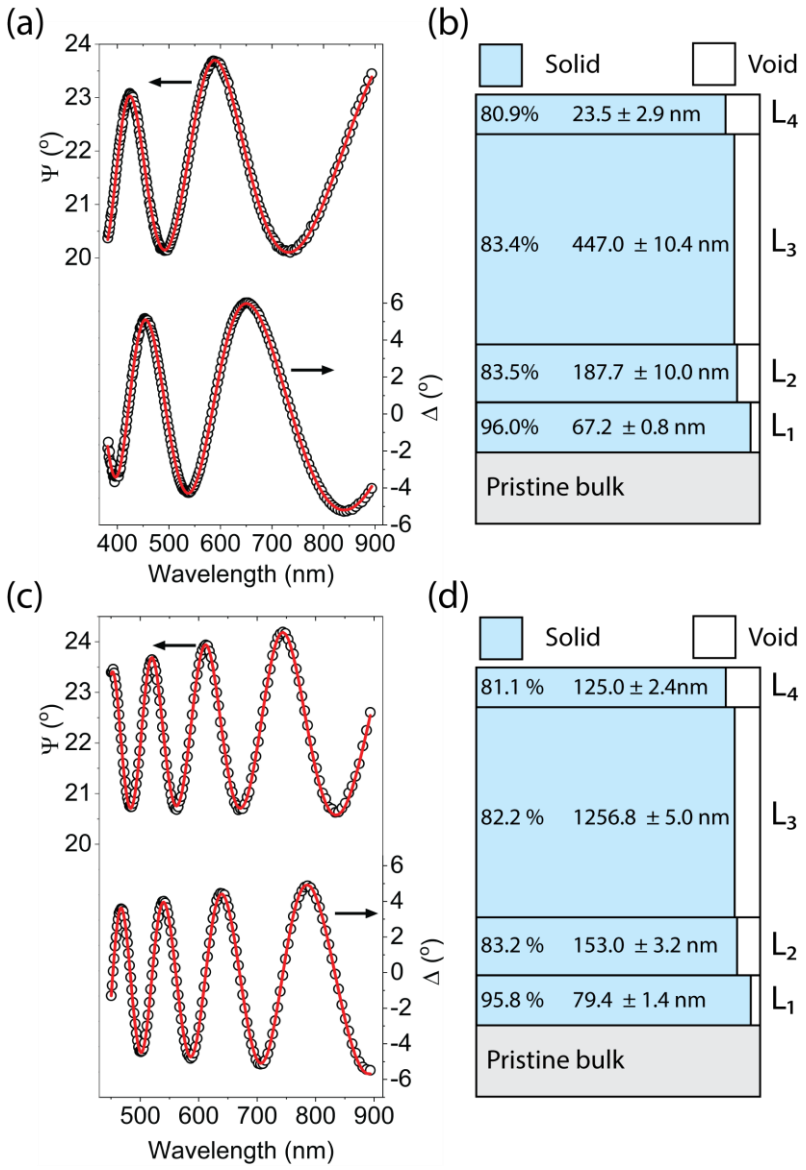

Figure 2. Analysis of the thickness and porosity of the alteration layer on ISG samples corroded for 7 days (a, b) and 209 days (c, d). (a) and (c) show the variation of ellipsometric angles (Ψ and Δ) as a function of wavelength at 0% RH. The symbols are the raw data and the solid lines are the fit results. (b) and (d) schematically illustrate the thickness and porosity of individual layers determined from fitting of the data shown in (a) and (c) with an optical model.

146

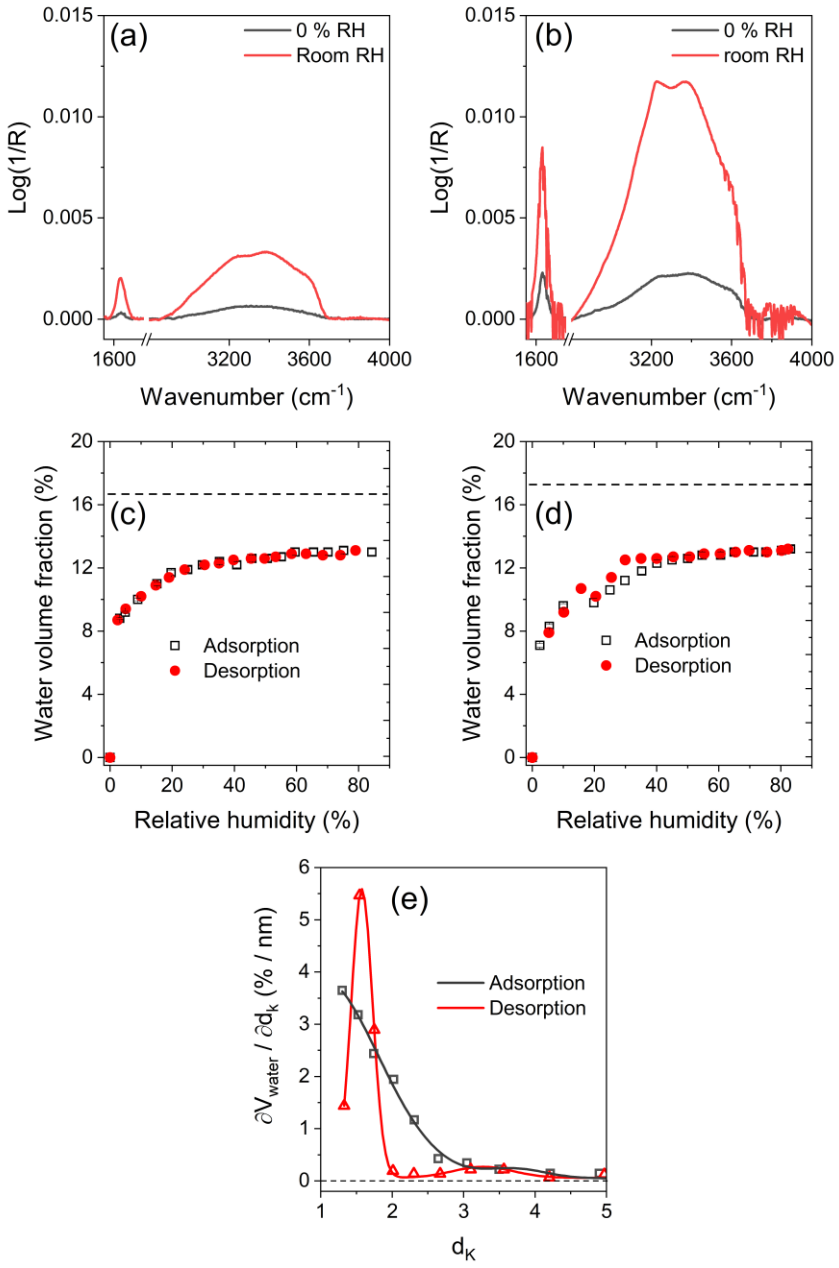

Figure 3. Uptake of water by the porous alteration layers formed by aqueous corrosion for 7 days (a, c) and 209 days (b, d). (a) and (b) are ATR-IR spectra of hydrous species in the porous alteration layer. (c) and (d) display the adsorption and desorption isotherms of water in the L_3 region of the alteration layer determined from SE as a function of RH. The 90% confidence intervals from the ellipsometry data analysis are shown in (c) and (d); but most of them are smaller than the symbol size. (e) Pore size distributions in the L_3 region of the alteration layer of 209-day corroded ISG sample calculated from (d). The symbols are the raw data and the smooth solid lines are added to show the overall trends.

The uptake of water from the surrounding gas phase can be confirmed using ATR-IR spectroscopy (Figures 3a and 3b). The intensities of the H_2O bending (~1650 cm^{-1}) mode and the OH stretching band (~2900-3700 cm^{-1}) at room RH (~40 %) are higher than those at 0% RH. Although the increase in the intensity of OH stretching band could be due to the increase in the abundance of silanol (SiOH) as well as molecular water, the intensity increase of the H_2O bending mode certainly indicates the amount of molecular water in the alteration layer is higher at room humidity than 0% RH. Although the elemental depth profile of the alteration layer of corroded ISG samples were reported by Gin et al. with SIMS under vacuum (Figure 3 of Ref. [5])[5], without knowing the depth profile of hydrogen species in hydrated state it is difficult to determine the relative abundance of the SiOH and H_2O species from the ATR-IR analysis.[39]

More quantitative information can be obtained by measuring the SE data as a function of RH. The changes in the ellipsometric angles (Ψ and Δ) measured at various RHs can be fitted using the same optical model constructed in the 0% RH case and allowing the volume fraction of pores filled with water. Figures 3c and 3d display the water volume fraction in the porous alteration layer determined while RH increases stepwise from 0% to 85% (adsorption) and then back to 0% (desorption). For the 7-day corroded ISG, the water adsorption/desorption isotherm follows the type-I behavior (Figure 3c).[29] This implies that the average pore size in the 7-day old alteration layer is <2 nm. This is in a good agreement with high-resolution transmission electron microscopy data published previously.[5] In the case of the 209-day corroded ISG, it follows the type-IV behavior of adsorption isotherm (Figure 3d). From the fact that the knee-shape kink of the type-IV isotherm occurs around 30-35 %RH, the presence of pores larger than 2 nm in the 209-day corroded ISG sample can be confirmed (Figure 3e).[33]

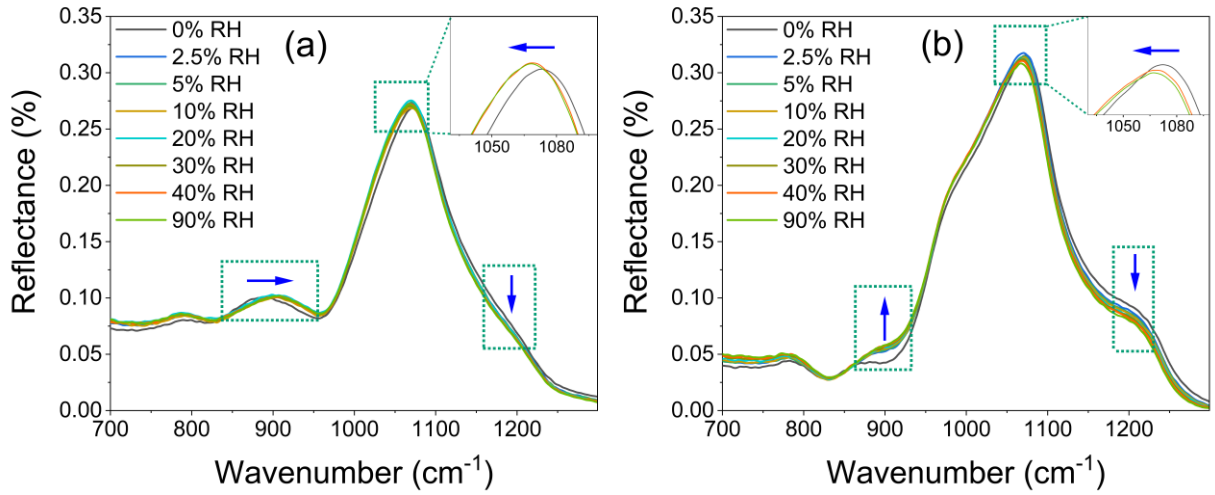

Figure 4. SR-IR spectra of the alteration layers on (a) 7-day corroded and (b) 209-day corroded ISG collected at various RH conditions. The SR-IR data of the uncorroded pristine glass is shown in the Supporting Information for comparison.

169

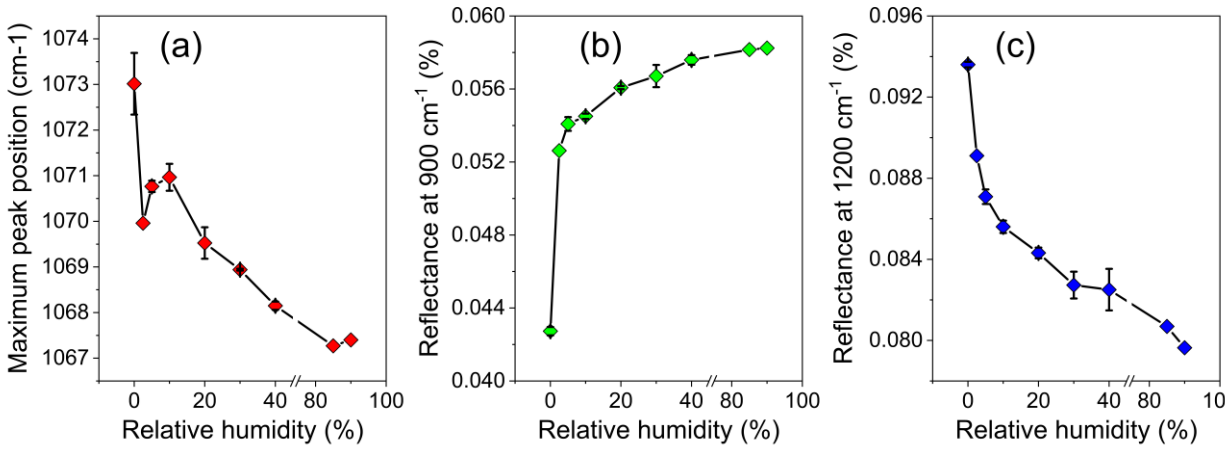

Figure 5. Changes in (a) main $\upsilon_{Si\text{-}O\text{-}Si}$ band position, (b) reflectance at 900 cm^{-1}, and (c) reflectance at 1200 cm^{-1} of the SR-IR spectra of 209-day corroded ISG glass as a function of RH in the surrounding environment. In (a), the position was determined from non-linear fit of the top part of the absorption band. The error bar is standard error of mean (N = 2).

The SR-IR spectra of these samples measured at different RH conditions are displayed in Figure 4. As the RH increases, the position of the main $\nu_{Si\text{-}O\text{-}Si}$ band shows a red-shift from 1072 cm^{-1} to 1068 cm^{-1}. The red-shift of the main band position is accompanied by a slight increase in the lower wavenumber shoulder and a slight decrease in the higher wavenumber shoulder. The detailed RH dependence of the main band position near 1070 cm^{-1}, the intensity at the lower wavenumber shoulder at 900 cm^{-1}, and the intensity at the high wavenumber shoulder at 1200 cm^{-1} are plotted in Figure 5 for the 209-day corroded ISG sample.

An apparent correlation can be seen between the water adsorption isotherms (Figure 3) and the RH dependence of the SR-IR spectral features (Figures 4 and 5). Based on the previous reports on swelling of porous Vycor glass[8, 9, 40] and MD simulation results published by Luo et al.,[26] one could attempt to attribute the 4 cm^{-1} shift in the $\nu_{Si\text{-}O\text{-}Si}$ band position (Figure 5a) to a strain of ~0.05 % in the average Si-O bond length. However, before such comparison is made, it is critically necessary to confirm that the observed spectral change with RH is not due to the change in effective refractive index of the porous medium upon filling of pores with water molecules; or, the change in effective refractive index effect must be properly subtracted from the observed result.

In order to calculate the spectral variation due to the change in effective refractive index of the porous alteration layer, the accurate data on its refractive index as a function of wavelength in the mid-IR region is needed. But, such data is not readily available because the composition and structure of the network in the alteration layer can vary depending on the initial composition of the bulk glass, the surface preparation before the corrosion, and the concentration, temperature, and time of the aqueous solution during the corrosion.[41, 42] Another complication would be the variation of porosity as a function of depth from the surface within the alteration layer (Figure 2). Also, the thickness of the alteration layer is smaller than the SR-IR probe depth which is on the

order of a micrometer at the peak of the $\nu_{Si\text{-}O\text{-}Si}$ band and varies over more than an order of magnitude even within the same band depending on the wavelength.[39, 43]

In order to check the effect of changes in effective refractive index of the porous layer without such complications, we have tested the RH dependence of the SR-IR spectral shape of the Vycor glass. Vycor is a highly-porous silica-rich glass obtained after dissolving the alkali borate-rich phase in a borosilicate glass.[44] Figure 6a shows the experimentally obtained SR-IR spectra of the Vycor glass at 0 % and 90 % RH conditions. The overall spectral changes are qualitatively similar to the trends observed for the porous alteration layers on ISG (Figures 4 and 5). Compared to the 0% RH data, the 90% RH spectrum shows a red-shift of the main absorption band position by ~1.4 cm^{-1} and an increase in the intensity at the 900 cm^{-1} and a decrease at the 1200 cm^{-1} regions.

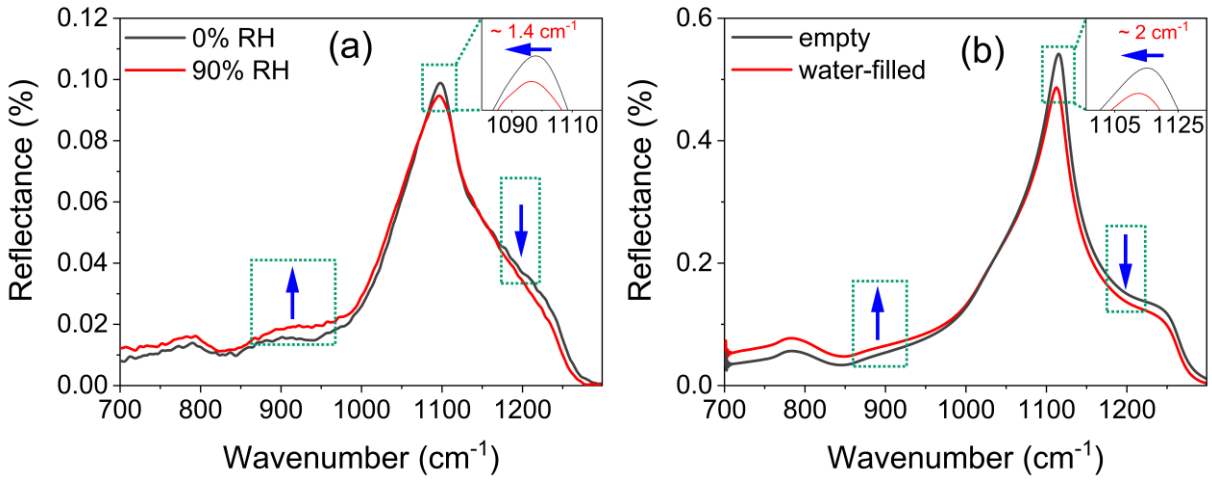

Figure 6. Comparison of (a) experimentally-observed changes of the SR-IR spectra of Vycor glass upon increase of RH from 0% to 90% and (b) theoretically-calculated SR-IR spectra of a medium consisting of 72% silica and 28% pores when pores are empty and filled water.

Although not accurate, the refractive index of silica[36] could be used for the solid part of the Vycor glass. The refractive index of water absorbed in the internal pores of the Vycor glass

206 could be assumed to be the same as that of liquid water. Figure 6b displays the SR-IR spectra
207 theoretically calculated using the effective refractive index for a composite model consisting of
208 72% silica and 28% void. When the pores are fully occupied with water, then the real (n) and
209 imaginary (k) parts of the refractive index of the medium vary accordingly and the peak position
210 and the shape of the SR-IR spectrum also vary. Although the quantitative magnitude is different,
211 the qualitative trend in the theoretical spectral features upon filling the pores with water (Figure
212 6b) is very similar to the experimentally-observed trend (Figure 6a).

213 The results shown in Figure 6 indicate that in SR-IR analysis of the porous alteration layer,
214 the ref-shift of the $\nu_{Si\text{-}O\text{-}Si}$ peak position (Figures 4 and 5a) as well as intensity changes in the lower
215 and upper region shoulders (Figures 5b and 5c) can originate from not only the adsorption-induced
216 stress to the glass network, but also the change in effective refractive index of the layer upon uptake
217 of water into the internal pores. It is interesting to note that the RH dependence of the position of
218 the maximum intensity (Figure 5a) is somewhat different from the water adsorption isotherm
219 (Figure 2d), while the shoulder intensities at 900 cm^{-1} and 1200 cm^{-1} regions (Figures 5b and 5c)
220 closely follow the isotherm data (Figure 2d). This may suggest that the peak (maximum intensity)
221 position of the Si-O-Si stretch band may be a convolution of both effects – adsorption-induced
222 stress and effective refractive index change. Deconvoluting those two effects would not be possible
223 without knowing the exact refractive index of the completely-dried alteration layer as a function
224 of depth from the surface.

225

Conclusions

Spectral changes in the Si-O-Si stretch band of the porous alteration layer on glass formed through aqueous corrosion are observed when the ambient relative humidity is varied. Although the peak position could be correlated with the theoretically predicted strain in the glass network, the experimentally observed spectral changes cannot be fully attributed to the adsorption-induced stress to the glass network. The ingress of water into internal pores of the subsurface region alters the effective refractive index of the sample, which will also modify the experimentally-observed IR spectral features. Deconvolution of these two effects is difficult without knowing the exact refractive index of the alteration layer in the Si-O-Si absorption band region.

Acknowledgements. This work was supported as part of the Center for Performance and Design of Nuclear Waste Forms and Containers, an Energy Frontier Research Center funded by the U.S. Department of Energy, Office of Science, Basic Energy Sciences under Award # DE-SC0016584. The authors thank Dr. Michael A. Hickner (The Pennsylvania State University) for the access to the spectroscopic ellipsometry setup in his lab.

References

[1] S. Wiederhorn, Influence of water vapor on crack propagation in soda-lime glass, Journal of the American Ceramic Society, 50 (1967) 407-414.
[2] R.H. Doremus, Diffusion of water in silica glass, Journal of Materials Research, 10 (1995) 2379-2389.
[3] T. Fett, K.G. Schell, M.J. Hoffmann, S.M. Wiederhorn, Effect of damage by hydroxyl generation on strength of silica fibers, Journal of the American Ceramic Society, 101 (2018) 2724-2726.
[4] T.A. Michalske, B.C. Bunker, K.D. Keefer, Mechanical properties and adhesion of hydrated glass surface layers, Journal of Non-Crystalline Solids, 120 (1990) 126-137.

[5] S. Gin, P. Jollivet, M. Fournier, F. Angeli, P. Frugier, T. Charpentier, Origin and consequences of silicate glass passivation by surface layers, Nat Commun, 6 (2015) 6360.
[6] K. Kinosita, Refractive Index and Pore Structure of Acid-Leached Surface Layer of Glass, Journal of the Physical Society of Japan, 16 (1961) 807-818.
[7] J.D. Vienna, J.V. Ryan, S. Gin, Y. Inagaki, Current Understanding and Remaining Challenges in Modeling Long-Term Degradation of Borosilicate Nuclear Waste Glasses, International Journal of Applied Glass Science, 4 (2013) 283-294.
[8] Y. Oka, J.M. Wahl, M. Tomozawa, Swelling and mechanical strength of glass, Journal of Non-Crystalline Solids, 38 & 39 (1980) 397-402.
[9] Y. Oka, J.M. Wahl, M. Tomozawa, Effect of Surface Energy on the Mechanical Strength of a High-Silica Glass, Journal of the American Ceramic Society, 64 (1981) 456-460.
[10] D.H. Bangham, N. Fakhoury, The swelling of charcoal. Part I.—Preliminary experiments with water vapour, carbon dioxide, ammonia, and sulphur dioxide, Proceedings of the Royal Society A, 130 (1930) 81-89.
[11] D.J.C. Yates, A Note on some Proposed Equations of State for, Proceedings of the Physical Society. Section B, 65 (1952) 80-81.
[12] G.Y. Gor, P. Huber, N. Bernstein, Adsorption-induced deformation of nanoporous materials—A review, Applied Physics Reviews, 4 (2017) 11303–11324.
[13] M. Nakamura, R. Kanzawa, K. Sakai, Stress and Density Effects on Infrared Absorption Spectra of Silicate Glass Films, Journal of the Electrochemical Society, 133 (1986) 1167-1171.
[14] M. Tomozawa, R.W. Hepburn, Surface structural relaxation of silica glass: a possible mechanism of mechanical fatigue, Journal of Non-Crystalline Solids, 345-346 (2004) 449-460.
[15] S.R. Ryu, M. Tomozawa, Fictive temperature measurement of amorphous SiO2 films by IR method, Journal of Non-Crystalline Solids, 352 (2006) 3929-3935.
[16] A. Agarwal, M. Tomozawa, Correlation of silica glass properties with the infrared spectra, Journal of Non-Crystalline Solids, 209 (1997) 166–174.
[17] G. Lucovsky, J.T. Fitch, E. Kobeda, E.A. Irene, Local Atomic Structure of Thermally Grown SiO2 Films, in: C.R. Helms, B.E. Deal (Eds.) The Physics and Chemistry of SiO 2 and the Si-SiO 2 Interface, Springer, 1988, pp. 139-148.
[18] J. Arndt, D. Stöffler, Anomalous changes in some properties of silica glass densified at very high pressures, Physics and Chemistry of Glasses, 10 (1969) 117-124.
[19] J.D. Mackenzie, High-pressure effects on oxide glasses: II, Subsequesnt heat treatment, Journal of The American Ceramic Society, 46 (1963) 470-476.
[20] Y.-K. Lee, Y.L. Peng, M. Tomozawa, IR reflection spectroscopy of a soda-lime glass surface during ion-exchange, Journal of Non-Crystalline Solids, 222 (1997) 125-130.
[21] N. Takamure, A. Kondyurin, D.R. McKenzie, Electric field assisted ion exchange of silver in soda-lime glass: A study of ion depletion layers and interactions with potassium, Journal of Applied Physics, 125 (2019) 175104-175116.
[22] J. Luo, W. Grisales, M. Rabii, C.G. Pantano, S.H. Kim, Differences in surface failure modes of soda lime silica glass under normal indentation versus tangential shear: A comparative study on Na+/K+-ion exchange effects, Journal of the American Ceramic Society, 102 (2019) 1665-1676.
[23] P. Innocenzi, Infrared spectroscopy of sol–gel derived silica-based films: a spectra-microstructure overview, Journal of Non-Crystalline Solids, 316 (2003) 309–319.
[24] P.N. Sen, M.F. Thorpe, Phonons inAX2glasses: From molecular to band-like modes, Physical Review B, 15 (1977) 4030-4038.

[25] F.L. Galeener, R.A. Barrio, E. Martinez, R.J. Elliott, Vibrational Decoupling of Rings in Amorphous Solids, Physical Review Letters, 53 (1984) 2429-2432.
[26] J. Luo, Y. Zhou, S.T. Milner, C.G. Pantano, S.H. Kim, Molecular dynamics study of correlations between IR peak position and bond parameters of silica and silicate glasses: Effects of temperature and stress, Journal of the American Ceramic Society, 101 (2018) 178-188.
[27] K.H. Nielsen, T. Kittel, K. Wondraczek, L. Wondraczek, Optical breathing of nano-porous antireflective coatings through adsorption and desorption of water, Sci Rep, 4 (2014) 6595.
[28] S. Gin, A. Abdelouas, L.J. Criscenti, W.L. Ebert, K. Ferrand, T. Geisler, M.T. Harrison, Y. Inagaki, S. Mitsui, K.T. Mueller, J.C. Marra, C.G. Pantano, E.M. Pierce, J.V. Ryan, J.M. Schofield, C.I. Steefel, J.D. Vienna, An international initiative on long-term behavior of high-level nuclear waste glass, Materials Today, 16 (2013) 243-248.
[29] D. Ngo, H. Liu, N. Sheth, R. Lopez-Hallman, N.J. Podraza, M. Collin, S. Gin, S.H. Kim, Spectroscopic ellipsometry study of thickness and porosity of the alteration layer formed on international simple glass surface in aqueous corrosion conditions, npj Materials Degradation, 2 (2018) 20.
[30] Corning, VYCOR® Brand Porous Glass 7930, in, 2001.
[31] P. Levitz, G. Ehret, S.K. Sinha, J.M. Drake, Porous vycor glass: The microstructure as probed by electron microscopy, direct energy transfer, small-angle scattering, and molecular adsorption, The Journal of Chemical Physics, 95 (1991) 6151-6161.
[32] F. Rouquerol, J. Rouquerol, K.S.W. Sing, G. Maurin, P. Llewellyn, Introduction, in: Adsorption by Powders and Porous Solids, 2014, pp. 1-24.
[33] S.J. Gregg, K.S.W. Sing, Adsorption, surface area, and porosity, 2nd ed., Academic Press, 1982.
[34] D.E. Aspnes, J.B. Theeten, F. Hottier, Investigation of effective-medium models of microscopic surface roughness by spectroscopic ellipsometry, Physical Review B, 20 (1979) 3292-3302.
[35] H. Fujiwara, Spectroscopic Ellipsometry, John Wiley & Sons, Ltd., 2007.
[36] I.H. Malitson, Interspecimen Comparison of the Refractive Index of Fused Silica, Journal of the Optical Society of America, 55 (1965) 1205-1209.
[37] M.E. Pemble, P. Gardner, Vibrational Spectroscopy from Surfaces, in: J.C. Vickerman, I.S. Gilmore (Eds.) Surface Analysis – The Principal Techniques, John Wiley & Sons, Ltd., 2009.
[38] D. Ngo, H. Liu, H. Kaya, Z. Chen, S.H. Kim, Dissolution of silica component of glass network at early stage of corrosion in initially silica-saturated solution, Journal of the American Ceramic Society, 0 (2019) 1-9.
[39] J. Luo, S.-i. Amma, L. Chen, D. Ngo, J.C. Mauro, C.G. Pantano, S.H. Kim, Relative abundance of subsurface hydroxyl and molecular water species in silicate and aluminosilicate glasses, Journal of Non-Crystalline Solids, 510 (2019) 179-185.
[40] C.H. Amberg, R. McIntosh, A study of adsorption hysteresis by means of length changes of a rod of porous glass, Canadian Journal of Chemistry, 30 (1952) 1012-1032.
[41] H. Liu, D. Ngo, M. Ren, J. Du, S.H. Kim, Effects of surface initial condition on aqueous corrosion of glass-A study with a model nuclear waste glass, Journal of the American Ceramic Society, 102 (2019) 1652-1664.
[42] L. Neill, S. Gin, T. Ducasse, T. De Echave, M. Fournier, P. Jollivet, A. Gourgiotis, N.A. Wall, Various effects of magnetite on international simple glass (ISG) dissolution: implications for the long-term durability of nuclear glasses, npj Materials Degradation, 1 (2017) 1.

[43] S.-i. Amma, J. Luo, C.G. Pantano, S.H. Kim, Specular reflectance (SR) and attenuated total reflectance (ATR) infrared (IR) spectroscopy of transparent flat glass surfaces: A case study for soda lime float glass, Journal of Non-Crystalline Solids, 428 (2015) 189-196.
[44] P. Wiltzius, F.S. Bates, S.B. Dierker, G.D. Wignall, Structure of porous Vycor glass, Physical Review A, 36 (1987) 2991-2994.